Chain Aggregation and Chain Collapse of Poly(methyl methacrylate) in a Mixed Solvent

Yoshiki Nakamura, Tomohide Nakagawa, Naoki Sasaki, Akihiko Yamagishi, and Mitsuo Nakata*

Department of Polymer Science, Faculty of Science, Hokkaido University, Sapporo 060-0810, Japan

Received January 12, 2001; Revised Manuscript Received May 17, 2001

ABSTRACT: Chain aggregation processes were studied for dilute solutions of PMMA with the molecular weight $m = 1.57 \times 10^6$ g/mol in the mixed solvent *tert*-butyl alcohol + water (2.5 vol %) at 25.0 and 30.0 °C in the concentration range from 1.4×10^{-4} to 5.7×10^{-4} g/cm^3. The weight-average molecular weight $\langle M\rangle_w$ and *z*-average squared radius $\langle R^2\rangle_z$ of clusters of polymer chains were determined as a function of time by static light-scattering measurements. The phase separation temperature increased from 35.7 to 36.7 °C in the concentration range. The aggregation process near the concentration $c = 1.46 \times 10^{-4}$ g/cm^3 was observed for a time period of about 10 000 min at 25.0 °C and 2000 min at 30.0 °C. At each temperature both the plots of $\ln\langle M\rangle_w$ and $\ln\langle R^2\rangle_z$ vs t (min) were represented by curved lines. The initial slopes of the lines were proportional to the concentration c. Accordingly, the scaled relations of $\langle M\rangle_w/M(0) = \exp(gct)$ and $\langle R^2\rangle_z/R^2(0) = \exp(hct)$ were obtained at small ct with $g = 5.01$ cm^3/(g min) and $h = 3.97$ cm^3/(g min) at 25.0 °C and with $g = 16.9$ and $h = 13.2$ at 30.0 °C, where $M(0)$ and $R^2(0)$ are the values extrapolated to $t = 0$. The reciprocals of gc and hc give the characteristic times of the chain aggregation. The longer characteristic times at 25.0 °C than at 30.0 were attributed to the effect of the chain collapse. The exponential growth indicated a reaction-limited cluster aggregation of polymer chains. The double-logarithmic plot of $\langle M\rangle_w$ vs $\langle R^2\rangle_z^{1/2}$ at each temperature was independent of concentration and represented by a single straight line with the slope $D = 2.53 \pm 0.02$ at 25.0 °C and 2.66 ± 0.01 at 30.0 °C.

1. Introduction

In dilute polymer solutions the coil−globule transition and phase separation occur competitively near the same temperature range. Since the two phenomena are caused by the interaction between polymer segments, they are intimately correlated with each other. Moreover, the kinetics of the chain collapse and phase separation may also reflect a common mechanism intrinsic to the polymer segment and solvent. At present it is important to disclose fundamental properties of the chain collapse and chain aggregation separately, though real polymer solutions may exhibit interesting behavior due to cooperativity of the coil−globule transition and phase separation. The characteristic time of phase separation depends on a specific nature of solution as well as the polymer concentration and molecular weight. For example, the phase separation appears to occur rapidly for polystyrene in cyclohexane[1] and very slowly for poly(*N*-isopropylacrylamide) in water.[2] We found that dilute solutions of poly(methyl methacrylate) (PMMA) underwent very slow phase separation and permitted us to study the coil−globule transition and phase separation process by light-scattering experiments.[3−6]

In previous studies,[4−7] we investigated the chain collapse process and chain aggregation process in dilute solutions of PMMA in isoamyl acetate by static light-scattering experiments. For an attainment of thermal equilibration, the light-scattering measurement was carried out 30 min after setting a solution cell in the photometer. On account of the blank time in the initial stage we employed solutions of high molecular weights, because the characteristic times of the chain collapse and phase separation processes for large molecular weight were much longer than the initial blank time. For the molecular weights $m = 2.35 \times 10^6$ g/mol and 4.4×10^6, the polymer chain collapsed to an equilibrium size about 30 min after quench, but the subsequent phase separation process was measured precisely.[7] For $m \times 10^{-6} = 8.4$ and 12.2 the chain collapse process was observed in a time period from several hundred minutes to a few thousand minutes, while the phase separation process was too slow to observe for an appropriate time period to experiment.[5]

The phase separation processes observed for $m \times 10^{-6} = 2.35$ and 4.4 were represented in terms of the weight-average molecular weight $\langle M\rangle_w$ and *z*-average radius $\langle R^2\rangle_z^{1/2}$ of clusters of polymer chains. The time evolution of a size distribution of clusters was expressed by an exponential growth as $\langle M\rangle_w \sim e^{Gt}$ and $\langle R^2\rangle_z \sim e^{Ht}$, where the coefficients G and H were proportional to the concentration. This behavior was in agreement with the Smoluchowski equation with the collision kernel $i + j$ for i-mer and j-mer[8,9] and was explained as due to a reaction-limited cluster aggregation (RLCA) rather than a diffusion-limited cluster aggregation (DLCA).[10] The double-logarithmic plot of $\langle M\rangle_w$ vs $\langle R^2\rangle_z^{1/2}$ was represented by a straight line with the slopes $D = 2.86 \pm 0.03$ and 3.06 ± 0.02 for $m \times 10^{-6} = 2.35$ and 4.4, respectively. The value of D was shown to be due to the structure of a cluster and size distribution of clusters. So far, we are not certain whether the above aggregation process of PMMA chains is specific to the solvent of isoamyl acetate or common to various solvents with different properties. To clarify this point, we searched for dilute PMMA solutions in which the solvent is somewhat peculiar and the chain aggregation occurs for an experimentally accessible time period.

In this paper, we studied chain aggregation processes for dilute solutions of PMMA in the mixed solvent *tert*-butyl alcohol + water (2.5 vol %). This mixed solvent may have a specific interaction with PMMA molecule, because both *tert*-butyl alcohol and water are nonsolvents for the polymer, but an addition of small amount of water to the alcohol gives rise to a strong solvent

10.1021/ma010064+ CCC: $20.00
Published on Web 07/10/2001

power for the polymer.[11] The θ-temperature of the solution of PMMA in the mixed solvent has been determined to be 41.5 °C.[3] The chain aggregation process was measured for the molecular weight $m = 1.57 \times 10^6$ at 25.0 and 30.0 °C. The coil−globule transition was completed in the first 30 min after quench, and the chain aggregation process was observed after the chain collapse for an appropriate time period to experiment. The experimental data were analyzed in a phenomenological way and were compared with those of the solution in isoamyl acetate to explore universal and specific features of the chain aggregation process. In a following paper, we determined the chain collapsing process of PMMA in the mixed solvent for $m \times 10^{-6} = 4.0$ and 12.2, taking advantage of the extremely slow aggregation process.[12]

2. Experimental Part

PMMA prepared by bulk polymerization was fractionated into 16 fractions (series M19), from which the sixth fraction M19-F6 with the weight-average molecular weight $m_w = 1.57 \times 10^6$ g/mol was used as a sample.[3] The characteristic ratio of the sample was observed to be $\langle s^2\rangle_z/m_w = 6.1 \times 10^{-4}$ nm^2 mol/g, which gave a measure for the molecular weight distribution as $m_w/m_n = 1.17$.[13] *tert*-Butyl alcohol was fractionally distilled immediately before use. Water was purified by a standard method.

The PMMA sample was dissolved in the mixed solvent *tert*-butyl alcohol (1) + water (2) at the volume fraction $u_2 = 0.025$ of water. The mixed solvent behaves as a single solvent in light scattering experiment, because the derivative dn/du_2 of the refractive index n of the solvent with respect to u_2 vanishes near $u_2 = 0.025$. The refractive index increment dn/dc (cm^3/g) at a relevant temperature t (°C) was estimated with the relation $dn/dc = 0.0994 + 3.2 \times 10^{-4}t$ at $u_2 = 0.025$.[3] It should be noticed that the volume fraction u_2 was used for *tert*-butyl alcohol in the mixed solvent in the previous study.

The static light-scattering measurements were carried out at an angular interval of 15° in the range from 30° to 150° with unpolarized incident light at 435.8 nm of a mercury arc as described elsewhere.[3,13] The chain aggregation process was determined at 25.0 and 30.0 °C. For the measurement at 25.0 °C, we prepared four solutions at the concentrations c (10^{-4} g/cm^3) = 1.464, 2.784, 4.257, and 5.694 in each optical cell of 18 mm i.d. and 1 mm wall thickness. At 30.0 °C we carried out measurements at four concentrations, c (10^{-4} g/cm^3) = 1.447, 2.745, 4.256, and 5.752, similar to the above concentrations. Optical clarification of the solutions was made with a Sartorius membrane filter (SM 116, 0.45 μm). Each solution cell was sealed tightly with a Teflon cap to prevent evaporation of the solvent and kept under the saturated vapor of the mixed solvent at the θ-temperature 41.5 °C in the dark. The optical cell was immersed in a thermostated cylindrical cell at the center in the photometer, and the measurement of scattered light was started 30 min after the quench on account of thermal equilibration. The chain aggregation process was pursued until the turbidity of the solution became perceptible to the eye. Thus, in the measurement the solution was transparent and multiple scattering effect was negligibly small.

The coil−globule transition curve was determined in the temperature region between 20 and 55 °C by light-scattering measurements carried out 30 min after setting solution.

To determine the molecular weight m, the mean-square radius of gyration $\langle s^2\rangle$, and the second virial coefficient A_2 for a single polymer, light-scattering data at an angle θ were transformed to the excess Raylaigh ratio R_θ and analyzed by the equation[14]

$$(Kc/R_\theta)^{1/2} = \{1/[mP_c(q)] + 2A_2c + ...\}^{1/2} \cong m^{-1/2}\{1 + (1/6)\langle s^2\rangle q^2 + mA_2c\} \quad (1)$$

with $K = (2\pi^2n^2/N_A\lambda^4)(dn/dc)^2$, $q = (4\pi n/\lambda)\sin(\theta/2)$, and $P_c(q)$ being the scattering function of a random flight polymer chain. Here, N_A is Avogadro's number, and λ is the wavelength of incident light in a vacuum. For polydisperse polymers m is the weight-average molecular weight, and $\langle s^2\rangle$ is the z-average mean-square radius of gyration.

An aggregation process of polymer chains may be expressed by a time evolution of cluster size distribution c_k, which denotes the concentration of k-mers. In the aggregation process, the concentration of total polymer is constant and given by the sum $c = \sum c_k$, where the summation is taken from the monomer $k = 1$ (single polymer chain). To simplify the problem, we assume that the polymer is monodisperse. Accordingly, R_θ is written as the sum $\sum Kc_kM_kP_k(q)$ with the molecular weight M_k ($=km$) and scattering function $P_k(q)$ for k-mer by neglecting the terms due to the virial coefficients. The optical constant K is independent of the cluster size k. Thus, we have

$$R_\theta/Kc = \langle M\rangle_w\langle P(q)\rangle_z \quad (2)$$

with

$$\langle M\rangle_w = \sum M_kc_k/\sum c_k \quad (3)$$

and

$$\langle P(q)\rangle_z = \sum P_k(q)M_kc_k/\sum M_kc_k \quad (4)$$

Here, $\langle M\rangle_w$ and $\langle P(q)\rangle_z$ are the weight-average molecular weight and z-average scattering function for clusters. For spherical particles, eq 2 can be expressed by the approximate form[15]

$$\ln(R_\theta/Kc) = \ln\langle M\rangle_w - (1/5)\langle R^2\rangle_z q^2 \quad (5)$$

where $\langle R^2\rangle_z$ is the z-average square radius of clusters. To determine $\langle M\rangle_w$ and $\langle R^2\rangle_z$ of clusters, light-scattering data were analyzed by the Guinier plot based on eq 5.

The phase separation temperature T_p of the solution was determined as the temperature at which scattered intensity began to increase on lowering temperature. The temperature was lowered by 0.1 K stepwise, and scattered intensities were monitored for a few days at each step. Thus, T_p (°C) was determined to be 35.7, 36.2, 36.6, and 36.7 at c (10^{-4} g/cm^3) = 1.43, 2.73, 4.17, and 5.58, respectively.

3. Experimental Results

Figure 1 shows the Berry−Zimm plots of light-scattering data according to eq 1. Plots a and b were obtained 30 min after setting the solution cell at the θ-temperature 41.5 and 25.0 °C, respectively. The values of m, $\langle s^2\rangle$, and A_2 were determined by the usual analysis due to eq 1. At the θ-temperature we obtained the characteristic ratio $\langle s^2\rangle_0/m = 6.1 \times 10^{-4}$ nm^2 mol/g. Figure 2 shows the temperature dependence of observed expansion factor $\alpha^2 = \langle s^2\rangle/\langle s^2\rangle_0$. Here, α^{-3} is plotted against temperature to highlight the behavior in the globule region. Figure 3 shows the temperature dependence of A_2.

Figure 4 represents the time evolution of scattered intensities from the solution at $c = 2.784 \times 10^{-4}$ g/cm^3 by the Guinier plot due to eq 5. The plots from the bottom to the top were obtained at 30, 300, 720, 1200, 1920, 2880, 3840, and 5340 min after quench to 25.0 °C. The values of $\langle M\rangle_w$ and $\langle R^2\rangle_z$ for polymer clusters at each time were determined from the intercept and the initial slope of the plot according to eq 5. Data at other concentrations were analyzed in the same way. Light-scattering data at 30.0 °C were also analyzed similarly.

Parts a and b of Figure 5 represent the semilogarithmic plots of $\langle M\rangle_w$ (g/mol) and $\langle R^2\rangle_z$ (nm^2) vs time t (min)

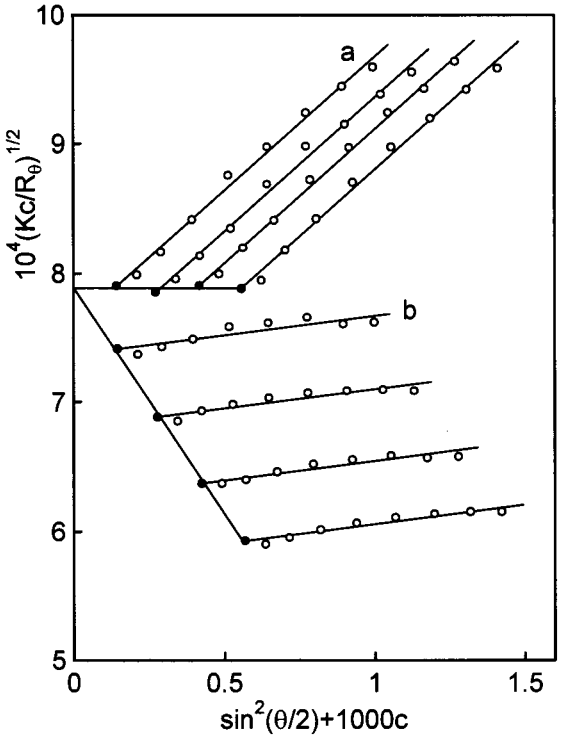

Figure 1. Berry−Zimm plots of the light-scattering data for PMMA in the mixed solvent *tert*-butyl alcohol + water (2.5 vol %). The data were obtained at 41.5 (a) and 25.0 °C (b) 30 min after setup the solution.

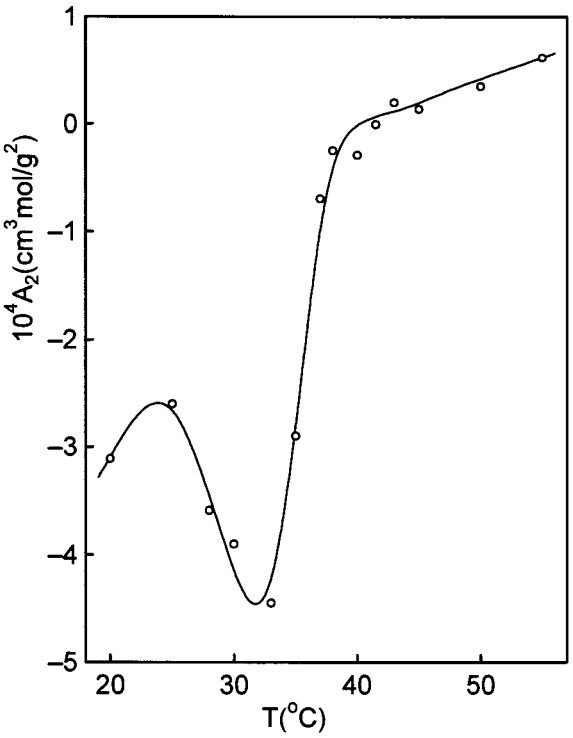

Figure 3. Temperature dependence of the second virial coefficient A_2 for PMMA in the mixed solvent *tert*-butyl alcohol + water (2.5 vol %) with the molecular weight $m = 1.57 \times 10^6$.

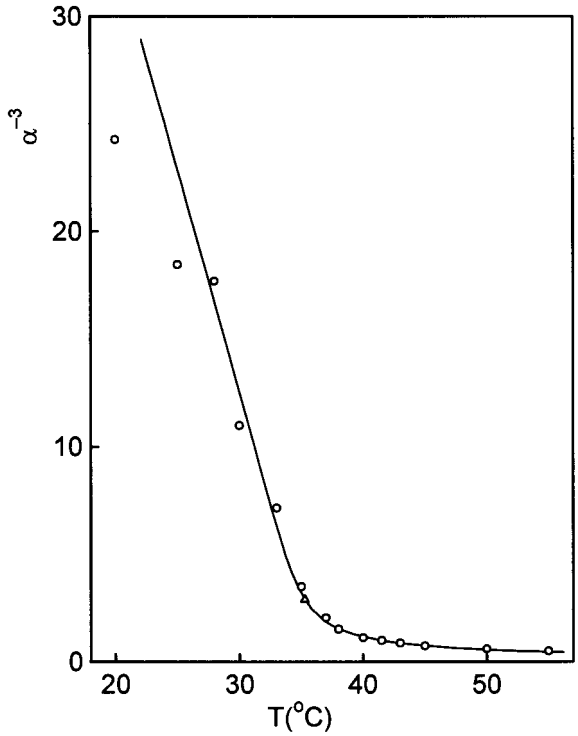

Figure 2. Coil−globule transition curve by plotting α^{-3} against temperature for PMMA in the mixed solvent *tert*-butyl alcohol + water (2.5 vol %) with the molecular weight $m = 1.57 \times 10^6$ g/mol. The triangle indicates the coil−globule crossover point determined as an inflection point of the curve $\alpha^2 = \alpha^2(\tau m^{1/2})$.

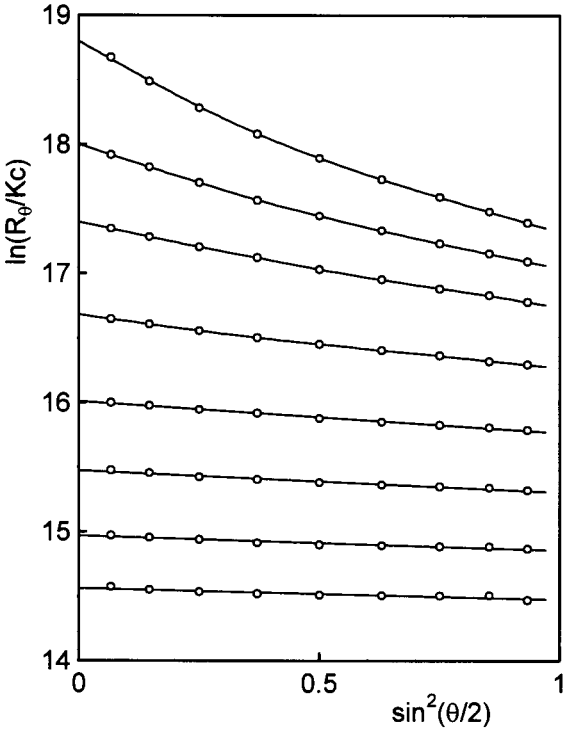

Figure 4. Scattered intensities from clusters of PMMA chains in the mixed solvent *tert*-butyl alcohol + water (2.5 vol %) at $c = 2.784 \times 10^{-4}$ g/cm^3. Guinier plots from the bottom to the top are made for data obtained 30, 300, 720, 1200, 1920, 2880, 3840, and 5340 min after quench to 25.0 °C.

at 25.0 °C, respectively. The different symbols are used to distinguish the data at different concentrations as c (10^{-4} g/cm^3) = 1.464 (○), 2.784 (△), 4.257 (□), and 5.694 (×). The inserted figures exhibit the initial processes in enlarged scale. Figures 6 represent the time evolutions of $\langle M\rangle_w$ and $\langle R^2\rangle_z$ at 30.0 °C in the same manner as in Figure 5. The data points were obtained at the concentrations as c (10^{-4} g/cm^3) = 1.447 (○), 2.745 (△),

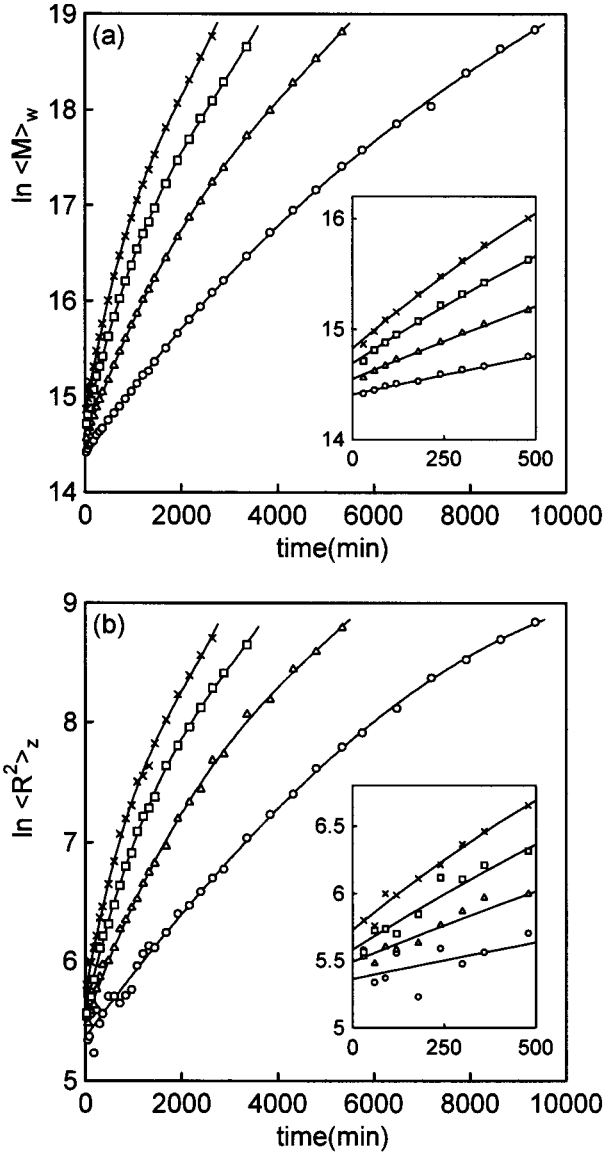

Figure 5. Time evolution of the weight-average molecular weight $\langle M\rangle_w$ (g/mol) and *z*-average square radius $\langle R^2\rangle_z$ (nm^2) of clusters of PMMA chains in the mixed solvent *tert*-butyl alcohol + water (2.5 vol %) at 25.0 °C. Plots of $\ln\langle M\rangle_w$ (a) and $\ln\langle R^2\rangle_z$ (b) vs *t* (min) were obtained at the concentrations *c* (10^{-4} g/cm^3) = 1.464 (○), 2.784 (△), 4.257 (□), and 5.694 (×).

4.256 (□), and 5.752 (×). Hereafter, we use the same symbols for data at each concentration and at each temperature.

Parts a and b of Figure 7 show the plot of $\ln\langle M\rangle_w$ vs $\ln\langle R^2\rangle_z^{1/2}$ at 25.0 and 30.0 °C, respectively. The symbols in Figure 7a,b are the same as those in Figures 5 and 6, respectively. At each temperature the data points construct a single straight line independent of time and concentration. Thus, the relation between $\langle M\rangle_w$ and $\langle R^2\rangle_z$ in the process of the chain aggregation can be expressed by the power law as

$$\langle R^2\rangle_z^{1/2} = A_p\langle M\rangle_w^{1/D} \tag{6}$$

By a least-squares fit, the exponent and coefficient were determined as $D = 2.53 \pm 0.02$ and $A_p = 0.050 \pm 0.001$ at 25.0 °C and $D = 2.66 \pm 0.01$ and $A_p = 0.074 \pm 0.001$ at 30.0 °C.

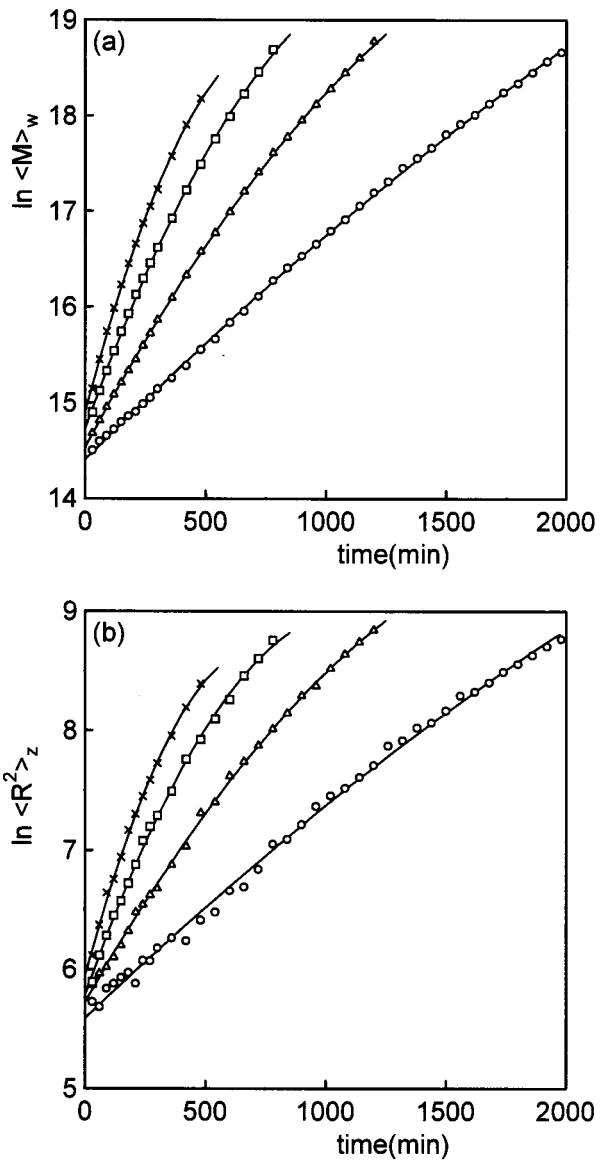

Figure 6. Time evolution of $\langle M\rangle_w$ (g/mol) and $\langle R^2\rangle_z$ (nm^2) at 30.0 °C as in Figure 5. Data points were obtained at the concentrations *c* (10^{-4} g/cm^3) = 1.447 (○), 2.745 (△), 4.256 (□), and 5.752 (×).

4. Discussion and Conclusion

The data points in Figure 2 were represented by the theoretical prediction[16]

$$\alpha^3 - \alpha - C(\alpha^{-3} - 1) = B\tau m^{1/2} \tag{7}$$

where τ is defined by $\tau = 1 - \theta/T$, and *B* and *C* are constants associated with the second and third virial coefficients for segment interactions, respectively. By using the linear plot of $(\alpha^3 - \alpha)/(\alpha^{-3} - 1)$ vs $\tau m^{1/2}/(\alpha^{-3} - 1)$, the values of *B* and *C* were determined to be $B = 0.0171$ and $C = 0.040$, which are close to the respective previous values.[3] In Figure 2, the solid line was calculated by using eq 7 with these values of *B* and *C*. As a coil−globule crossover point, the inflection point on the line $\alpha^2 = \alpha^2(\tau m^{1/2})$ was calculated by using eq 7 and obtained to be 35.3 °C and $\alpha^2 = 0.492$ as shown by the triangle. The solid line curves abruptly near the triangle, and the globule state is represented by the nearly straight line. The deviation of the data points from the straight line is caused by an experimental uncertainty

Table 1. Coefficients in Eqs 8 and 9 at 25.0 (i) and 30.0 °C (ii)[a]

(i) $T = 25.0$ °C

c (10^{-4} g/cm^3)	a_0	a_1 (10^{-3} min^{-1})	a_2 (10^{-7} min^{-2})	a_3 (10^{-10} min^{-3})	a_1/c (cm^3/(g min))	a_2/c^2 (cm^6/(g^2 min^2))	a_3/c^3 (cm^9/(g^3 min^3))	$M(0)$ (10^6 g/mol)
1.464	14.407	0.718	−0.348	0.009	4.91	−1.62	0.29	1.81
2.784	14.549	1.401	−1.771	0.121	5.03	−2.28	0.56	2.08
4.257	14.691	2.170	−4.845	0.569	5.10	−2.67	0.74	2.40
5.694	14.824	2.836	−8.511	1.309	4.98	−2.63	0.71	2.74

c (10^{-4} g/cm^3)	b_0	b_1 (10^{-3} min^{-1})	b_2 (10^{-7} min^{-2})	b_3 (10^{-10} min^{-3})	b_1/c (cm^3/(g min))	b_2/c^2 (cm^6/(g^2 min^2))	b_3/c^3 (cm^9/(g^3 min^3))	$R^2(0)$ (nm^2)
1.464	5.361	0.553	−0.173	−0.002	3.78	−0.81	−0.07	213
2.784	5.488	1.123	−1.405	0.087	4.03	−1.81	0.40	242
4.257	5.579	1.749	−3.877	0.418	4.11	−2.14	0.54	265
5.694	5.726	2.261	−7.224	1.125	3.97	−2.23	0.61	307

(ii) $T = 30.0$ °C

c (10^{-4} g/cm^3)	a_0	a_1 (10^{-3} min^{-1})	a_2 (10^{-7} min^{-2})	a_1/c (cm^3/(g min))	a_2/c^2 (cm^6/(g^2 min^2))	$M(0)$ (10^6 g/mol)
1.447	14.407	2.509	−0.173	17.34	−8.28	1.81
2.745	14.536	4.679	−0.970	17.05	−12.87	2.06
4.256	14.727	7.043	−2.583	16.55	−14.26	2.49
5.752	14.902	9.575	−5.795	16.65	−17.52	2.96

c (10^{-4} g/cm^3)	b_0	b_1 (10^{-3} min^{-1})	b_2 (10^{-7} min^{-2})	b_1/c (cm^3/(g min))	b_2/c^2 (cm^6/(g^2 min^2))	$R^2(0)$ (nm^2)
1.447	5.589	1.923	−0.143	13.29	−6.84	267
2.745	5.720	3.574	−0.809	13.02	−10.74	305
4.256	5.780	5.746	−2.549	13.50	−14.07	324
5.752	5.939	7.534	−5.148	13.10	−15.56	380

[a] The ratios of $a_i/c^i$and b_i/c^i were taken to examine scaled relations. $M(0)$ and $R^2(0)$ in the last column are equal to $\exp(a_0)$ and $\exp(b_0)$, respectively.

due to the small values of $\langle s^2\rangle$. It should be noticed that A_2 shown in Figure 3 yields a minimum near the coil−globule crossover point as predicted by a theoretical calculation in which the chain collapse was taken into account with the mean-field approximation.[17] The minimum in A_2 has been also observed near the coil−globule crossover point for the same solution with different molecular weights[3,12] and for the solution of PMMA in isoamyl acetate.[4]

The plots of $\ln\langle M\rangle_w$ and $\ln\langle R^2\rangle_z$ vs the time t given in Figures 5 and 6 were analyzed by the polynomials

$$\ln\langle M\rangle_w = a_0 + a_1 t + a_2 t^2 + a_3 t^3 \quad (8)$$

$$\ln\langle R^2\rangle_z = b_0 + b_1 t + b_2 t^2 + b_3 t^3 \quad (9)$$

The considerably curved plots in Figure 5 were well fitted to the above equations, while the slightly curved plots in Figure 6 were represented by the quadratic equations. Table 1 gives the obtained values of the coefficients a_i and b_i and the ratios of a_i/c^i and b_i/c^i. The last column gives the initial values of $\langle M\rangle_w$ and $\langle R^2\rangle_z$ estimated by $M(0) = \exp(a_0)$ and $R^2(0) = \exp(b_0)$. The lines in Figures 5 and 6 are described by the equations with the values of a_i and b_i in Table 1. Each line fits to the data points satisfactorily in the whole range of the time. The values of $M(0)$ and $R^2(0)$ extrapolated to zero time were compared reasonably with those of the molecular weight and mean-square radius of gyration $\langle s^2\rangle$ of the single polymer chain. The good fit of eqs 8 and 9 to the data points demonstrates that the chain aggregation started just after the quench without lag time, irrespective of the concentration and temperature. This implies that a cluster grows continuously from a single polymer chain without an incubation time. This continuous growth of cluster does not occur in the nucleation processes in usual low molecular weight liquids because of the free energy barrier to molecule aggregation, though the nucleus may be too small for the determination of the size. Raos and Allegra estimated the segment density of a single polymer below the chain collapse temperature to be as large as that of a critical nucleus.[18,19] Consequently, the free energy barrier to chain aggregation vanishes in the temperature region and the spinodal practically coincides with the binodal. The observed aggregation process without a critical nucleus may be compatible with this theoretical argument.

Each value of a_1/c and b_1/c in Table 1 is constant independent of the concentration at both 25.0 and 30.0 °C. The absolute values of $|a_i/c^i|$ and $|b_i/c^i|$ for $i = 2$ and 3 tend to increase with increasing concentration, and the absolute values at the lowest concentration seem to be exceptionally small. We made the scaled plots of $\ln\{\langle M\rangle_w/M(0)\}$ and $\ln\{\langle R^2\rangle_z/R(0)\}$ vs ct on account of the constant values of a_1/c and b_1/c. Figures 8 and 9 show the scaled plots at 25.0 and 30.0 °C, respectively. As anticipated, the plots give composite lines in the initial ranges of $\ln\{\langle M\rangle_w/M(0)\} < 1.5$ and $\ln\{\langle R^2\rangle_z/R(0)\} < 1$ at both the temperatures. In the range, the plots at 25.0 °C appear to be curved, while the plots at 30.0 °C appear to be linear. The straight lines in Figures 8 and 9 are given by the equations

$$\langle M\rangle_w/M(0) = \exp(gct) \quad (10)$$

$$\langle R^2\rangle_z/R^2(0) = \exp(hct) \quad (11)$$

where the coefficients g and h were estimated to be $g = 5.01$ cm^3/(g min) and $h = 3.97$ cm^3/(g min) at 25.0 °C and $g = 16.9$ and $h = 13.2$ at 30.0 °C by using the relations $g = a_1/c$ and $h = b_1/c$ and taking average over

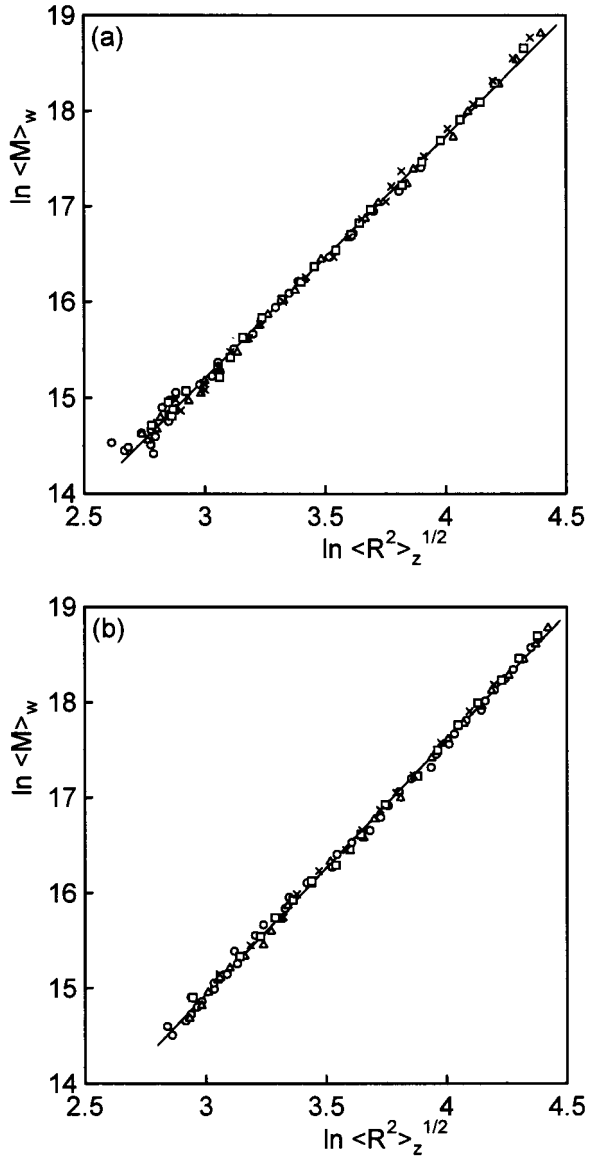

Figure 7. Double-logarithmic plot of $\langle M\rangle_w$ (g/mol) vs $\langle R^2\rangle_z^{1/2}$ (nm) at 25.0 (a) and 30.0 °C (b). The symbols in (a) and (b) are the same as in Figures 5 and 6, respectively.

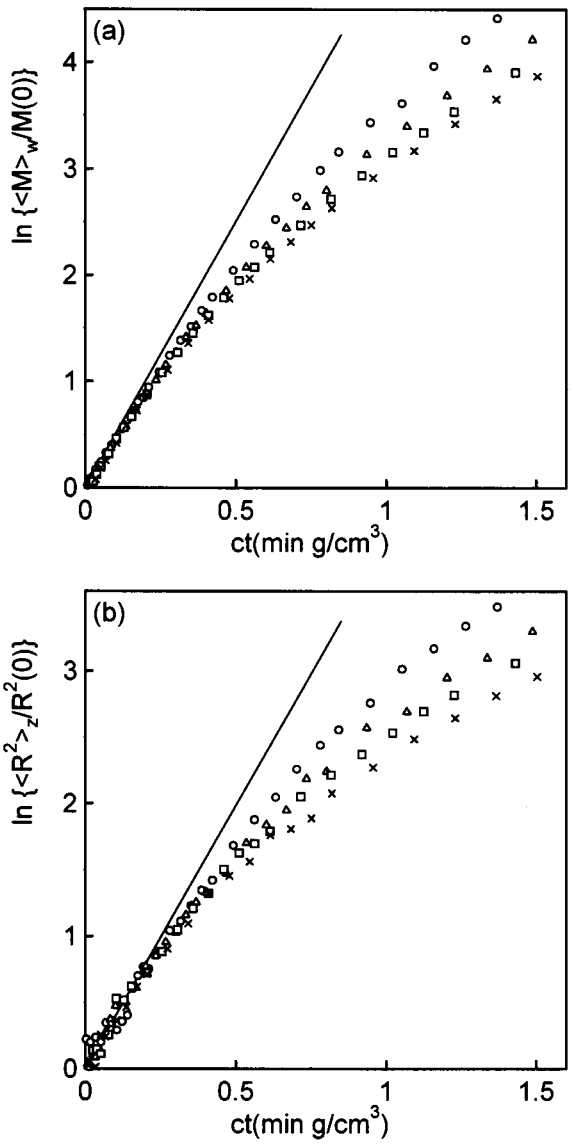

Figure 8. Plots for time evolution of $\langle M\rangle_w$ (a) and $\langle R^2\rangle_z$ (b) with scaled variables at 25.0 °C. The symbols are the same as in Figures 5. The straight line indicates the initial slope obtained as an average of those at each concentration.

the concentration. The data points at large *ct* in each plot show larger deviation from the straight line with increasing concentration. It is interesting to observe that each composite line at small *ct* begins to separate near $\ln\{\langle M\rangle_w/M(0)\} = 1.5$ or $\ln\{\langle R^2\rangle_z/R(0)\} = 1$ depending on the concentration. The separation occurs in accordance with a rule which gives rise to the composite lines in Figures 7. It should be noticed that the value of $\ln\{\langle M\rangle_w/M(0)\} = 1.5$ yields the weight-average number of polymer chains in a cluster as $\langle M\rangle_w/M(0) = 4.5$. Thus, the composite lines in Figures 8 and 9 are obtained in a region of small size cluster. At large *ct*, the plots in Figures 8a and 9a extend to near $\ln\{\langle M\rangle_w/M(0)\} = 4$, that is, $\langle M\rangle_w/M(0) = 60$.

As indicated by the time scale in Figures 5 and 6, the chain aggregation occurs much faster at 30.0 °C than at 25.0 °C. According to eqs 10 and 11, the reciprocals of *gc* and *hc* indicate the characteristic times of chain aggregation at small *ct*. The ratio of *gc* at 25.0 °C to that at 30.0 °C as well as the similar ratio for *hc* is estimated as 3.3. Since the phase separation temperature has been observed between 35.7 and 36.7 °C in the present concentration range, the chain aggregation process is faster near 6 K below the phase separation temperature than near 11 K. In general, a phase separation process is faster at a larger temperature distance from the phase separation temperature. This is not the case for the present phase separation. However, in Figure 3, A_2 yields a maximum and minimum near 25.0 and 30.0 °C, respectively, and are compatible with the inverted rate of the chain aggregation. The PMMA chain is in the globule state at both 25.0 and 30.0 °C on account of the crossover temperature 35.3 °C. According to Figure 2, the size of the globule is considerably different at these temperatures. Thus, the inverted rate of the chain aggregation has a subtle correlation with the size of polymer chain.

Smoluchowski formulated aggregation kinetics in terms of cluster−cluster collisions. A *k*-mer can be formed by a collision of *i*-mer and *j*-mer ($k = i + j$) and converted into a larger size cluster by collisions with other clusters.[8,9] By assuming a random distribution of clusters in solution, the time evolution of the number $N_k(t)$ of *k*-mer ($k = 1, 2, ...$) in unit volume was expressed

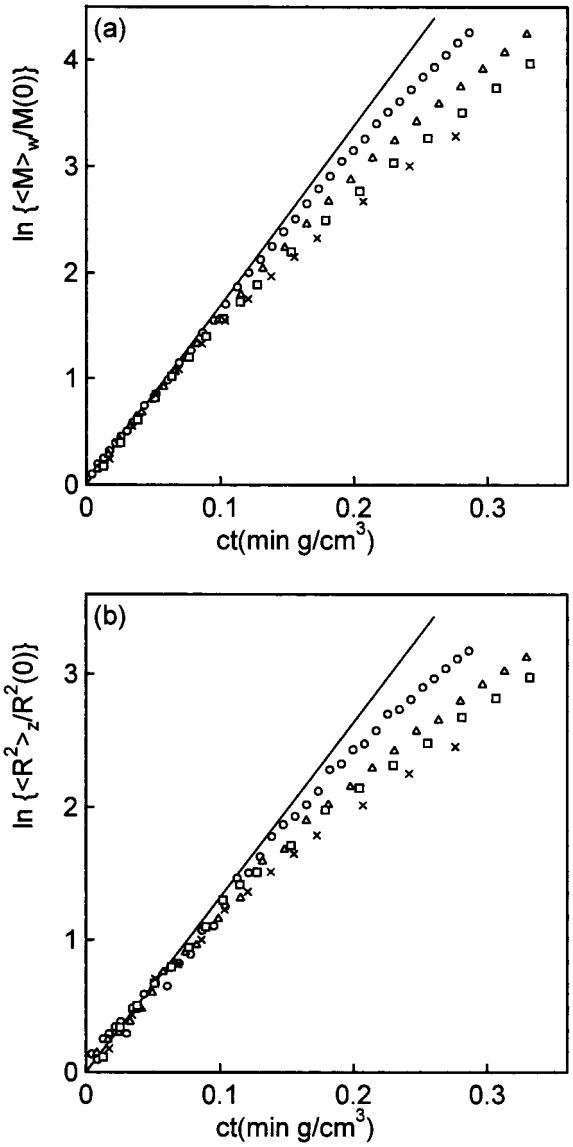

Figure 9. Plots for time evolution of $\langle M\rangle_w$ (a) and $\langle R^2\rangle_z$ (b) at 30.0 °C as in Figure 8. The symbols are the same as in Figure 6.

with the collision kernel K_{ij} in the form

$$dN_k/dt = {}^1/_2 \sum_{i+j=k} K_{ij}N_iN_j - N_k \sum_j K_{kj}N_j \quad (12)$$

Equation 12 has been solved only for $K_{ij} = 1$, $i + j$, and $i \times j$ and their linear combinations, while the moments of the distribution defined by $Q_n(t) = \sum k^n N_k(t)$ can be easily calculated by[20,21]

$$dQ_n/dt = {}^1/_2 \sum_i \sum_j [(i+j)^n - i^n - j^n]K_{ij}N_iN_j \quad (13)$$

The moment Q_1 represents the total number N of monomers and should be constant. The number-average molecular weight and weight-average molecular weight of clusters are represented by $\langle M\rangle_n = mQ_1/Q_0$ and $\langle M\rangle_w = mQ_2/Q_1$, respectively. The time evolution of $Q_n(t)$ can be obtained explicitly for a given form of K_{ij} and initial condition. In the present experiment, the initial condition is given by $N_1(0) = N$ $(=c/m)$, and $N_i(0) = 0$ $(i \geq 2)$. For the diffusion-limited cluster aggregation (DLCA), the collision kernel is constant independent of i and j and given by $K_{ij} = 8\pi D_t R$, where D_t and R are the diffusion constant and radius of a monomer, respectively.[9] For DLCA, we have

$$\langle M\rangle_w = m(1 + 8\pi D_t Rct/m) \quad (14)$$

which gives a characteristic time as $1/(8\pi D_t RN)$. Using the Stokes−Einstein relation $D_t = kT/(6\pi\eta R)$, the characteristic time is written as $3\eta/4kTN$. Here, η is the viscosity coefficient and roughly 10^{-3} Pa·s for the present mixed solvent. Thus, the characteristic time is estimated to be 10^{-2} s in the experimental concentration range and is several orders smaller than the time period of the observed chain aggregation process.

For the collision kernel $K_{ij} = B(i + j)$ with B as a constant, we have

$$\langle M\rangle_w = m \exp(2Bct/m) \quad (15)$$

The exponential growth of cluster has been known to be caused by the reaction-limited cluster aggregation (RLCA).[10,22] The observed chain aggregation processes has the same form as eq 15 in a functional form and in a scaled form with ct as a variable. Thus, we have $g = 2B/m$. The temperature dependence of g is included phenomenologically in B. In a following paper for PMMA chain collapse,[12] the collapse process was found to be slower for higher molecular weights. For $m = 1.22 \times 10^7$, the chain collapse process to an equilibrium size was observed for a time period of several days, and the chain aggregation was anticipated to occur after the chain collapse. It is obvious that the time period of chain aggregation process for $m = 1.22 \times 10^7$ is much longer than that for $m = 1.57 \times 10^6$. Thus, g is expected to decrease with increasing molecular weight.

In previous studies,[6,7] chain aggregation processes were measured for PMMA in isoamyl acetate with $m = 2.35 \times 10^6$ at 25.0 °C and with $m = 4.4 \times 10^6$ and at 30.0 °C. Each plot of $\ln\{\langle M\rangle_w/M(0)\}$ and $\ln\{\langle R^2\rangle_z/R^2(0)\}$ vs ct was represented by a single straight line for both the molecular weights. The relation between $\langle M\rangle_w$ and $\langle R^2\rangle_z$ was described by eq 6 with $D = 2.86 \pm 0.03$ for $m = 2.35 \times 10^6$ and $D = 3.06 \pm 0.02$ for $m = 4.4 \times 10^6$. The chain aggregation processes in the form of eqs 10 and 11 were compared with the Smoluchowski equation with the collision kernel $K_{ij} = B(i + j)$, and the coefficient B was determined. Thus, the Smoluchowski equation was used to analyze the chain aggregation process and revealed that the exponent D was caused by the time evolution of the cluster size distribution and by the size dependence of the structure of cluster. For small size clusters the segment density of a cluster increased with increasing cluster size. In light of this analysis the constant values of D obtained in the present study may be attributed to the size distribution of clusters and the size dependence of the cluster structure, though the aggregation processes shown in Figures 8a and 9a satisfy eq 15 at small ct and deviate appreciably from it at large ct. The Smoluchowski equation can give a reliable analysis for aggregation processes expressed properly by eq 15 and may disclose the structure of cluster. Recently, we observed that the present PMMA solution exhibited the aggregation process expressed by eq 15 at a temperature above 30 °C.

The PMMA solutions in isoamyl acetate and in the present mixed solvent are very different in equilibrium properties. The coil−globule transition curve in isoamyl acetate was represented by eq 7 with $B = 0.0041$ and C

$= 0.073$,[4] which are considerably different from the corresponding values in the mixed solvent. Water in the mixed solvent may play a particular role for miscibility of PMMA. However, the cluster growth processes of PMMA chains in isoamyl acetate and the mixed solvent are essentially similar in the time and concentration dependences and are dominated by RLCA. Furthermore, the relation between $\langle M \rangle_w$ and $\langle R^2 \rangle_z$ is independent of the concentration. Thus, the aggregation process observed in this study may reflect a common feature in the cluster formation of PMMA chains. Equation 15 seems to be satisfied rather in limited ranges of temperature, molecular weight, and concentration.

References and Notes

(1) Chu, B.; Ying, Q.; Grosberg, A. Y. *Macromolecules* **1995**, *28*, 180.
(2) Wang, X.; Qiu, X.; Wu, C. *Macromolecules* **1998**, *31*, 2972.
(3) Nakata, M. *Phys. Rev. E* **1995**, *51*, 5770.
(4) Nakata, M.; Nakagawa, T. *Phys. Rev. E* **1997**, *56*, 3338.
(5) Nakata, M.; Nakagawa, T. *J. Chem. Phys.* **1999**, *110*, 2703.
(6) Nakata, M.; Nakagawa, T.; Nakamura, Y.; Wakatsuki, S. *J. Chem. Phys.* **1999**, *110*, 2711.
(7) Nakagawa, T.; Nakamura, Y.; Sasaki, N.; Nakata, M. *Phys. Rev. E* **2001**, *63*, 031803.
(8) Smoluchowski, M. V. *Z. Phys. Chem. (Muenchen)* **1917**, *92*, 129; *Phys. Z.* **1916**, *17*, 585.
(9) Chandrasekhar, S. *Rev. Mod. Phys.* **1943**, *15*, 1.
(10) Vicsek, T. In *Fractal Growth Phenomena*; Word Scientific: Singapore, 1989.
(11) Cowie, J. M. G.; Mohsin, M. A.; McEwen, I. J. *Polymer* **1987**, *28*, 1569.
(12) Nakamura, Y.; Sasaki, N.; Nakata, M. *Macromolecules* **2001**, *34*, 5992 (following paper).
(13) Nakata, M.; Kawate, K.; Ishitaka, Y. *Macromolecules* **1994**, *27*, 1825.
(14) Nakata, M. *Polymer* **1997**, *38*, 9.
(15) Turkevich, J.; Hubbell, H. H. *J. Am. Chem. Soc.* **1951**, *73*, 1.
(16) Birshtein, T. M.; Pryamitsyn, V. A. *Macromoleclues* **1991**, *24*, 1554.
(17) Tanaka, F. *J. Chem. Phys.* **1985**, *82*, 4707.
(18) Raos, G.; Allegra, G. *Macromolecules* **1996**, *29*, 6663.
(19) Raos, G.; Allegra, G. *J. Chem. Phys.* **1997**, *107*, 6479.
(20) Ziff, R. M. In *Kinetics of Aggregation and Gelation*; Family, F., Landau, D. P., Eds.; North-Holland: Amsterdam, 1984.
(21) Cohen, R. J.; Benedek, G. B. *J. Phys. Chem.* **1982**, *86*, 3696.
(22) Lin, M. Y.; Klein, R.; Lindsay, H. M.; Weitz, D. A.; Ball, R. C.; Meakin, P. J. *Colloid Interface Sci.* **1990**, *137*, 263.

MA010064+